RESEARCH ARTICLE

Editorial Process: Submission:09/08/2025 Acceptance:02/17/2026 Published:03/05/2026

Impact of Optimization Resolution and Dose Calculation Grid Size in Small-Field Stereotactic Body Radiotherapy Using Flattening-Filter-Free Beams for Hepatocellular Carcinoma

Moorthi Thirunavukarasu[1,2]*, D Khanna[1], Karunakaran Balaji[3], Mohan Ramachandran[4]

Abstract

Objective: This study aims to evaluate the impact of optimization and calculation resolutions in SBRT for hepatocellular carcinoma (HCC) using flattening-filter-free photon beams. **Methods:** The SBRT plans were created in the Eclipse TPS using 6X-FFF and 10X-FFF MV photon beams, prescribed with a hypofractionated dose of 50 Gy in 5 fractions. A total of 4 plans were created for each energy with different combinations of optimization (O) and calculation (C) resolutions, viz. O1.25-C1.25, O1.25-C2.5, O2.5-C1.25, and O2.5-C2.5, using computed tomography (CT) images of fifteen HCC patients. The optimization and calculation times were noted for comparison among all plans. The plans were evaluated based on the PTV, organs at risk, and delivery efficiency dosimetric parameters, and a plan quality score was computed for each plan. **Results:** This study revealed that the 10X-FFF beams provided better results compared to 6X-FFF. The integrated scoring method revealed that the O1.25-C1.25 plan achieved better results for OARs, while O1.25-C2.5 plan achieved better results for PTV. Further, the optimization and calculation times, and phantom study results were better with 2.5 mm resolution plans. **Conclusion:** The 1.25 mm resolution for both optimization and calculation was found to be better if the critical organs are in prioritized; otherwise, the 2.5 mm resolution setting is the optimal choice for liver SBRT using the 10X-FFF beam.

Keywords: liver cancer- SBRT- FFF- VMAT- calculation resolution

Asian Pac J Cancer Prev, **27 (3)**, 1115-1121

Introduction

The global cancer observatory reports in 2022 show that the hepatocellular carcinoma (HCC) incidence rate is 4.3% (sixth position) and the mortality rate is 7.8% (third position) among all cancers worldwide [1]. Radiotherapy is an advisable treatment choice for HCC, predominantly for patients who are not able to endure surgery [2]. Stereotactic body radiation therapy (SBRT) has become more operative than conventionally fractionated radiotherapy in increasing local tumor control of primary and metastatic liver tumors, predominantly in patients with small tumors [3-7].

The correlation between exposed normal liver volume and toxicity is a foremost apprehension for radiation-induced liver disease (RILD) during radiotherapy of HCC [8]. The SBRT of HCC has been made more pertinent by the evolution of radiotherapy techniques, mainly volumetric modulated arc therapy (VMAT) and enhanced image guidance methods, with reassuring results. Nevertheless, the use of high-precision techniques required utmost care in delivering a high dose of radiation to the target and upholding a rapid fall-off dose from the target. In that way it will attain extreme treatment efficacy with minimal toxicity to normal tissues. In order to accomplish this, a treatment planning system (TPS) with advanced dose computation algorithms is essential.

The TPS gets a 3D dose distribution on patient's computed tomography (CT) images by interpolating the dose between adjacent calculation grid points. When the calculation grid size is big, the volume averaging effect may upshot in uncertainties [9]. Dose calculation resolution has been inspected in several studies to determine its impact on the accuracy of calculated dose distributions. For instance, Huang et al. and Park et al. appraised the impact of calculation grid size in lung SBRT [10, 11]. Similarly, Snyder Karen et al. evaluated the impact of calculation grid size in spine SBRT, and Park et al. in conventional head and neck plans [12, 13]. Different grid sizes have been recommended by these studies for dose calculation. Chung et al., have shown that the dose variations are influenced by the size of the

*[1]Department of Physics, Karunya Institute of Technology and Sciences, Coimbatore, India. [2]Department of Radiation Oncology, Gleneagles Hospitals, Chennai, India. [3]Department of Oncology, Iswarya Hospital, Chennai, India. [4]Mediclinic Middle East, Dubai Healthcare City, Dubai, United Arab Emirates. *For Correspondence: moorthiuts@gmail.com*

calculation grid [14].

The impact of calculation grid size on liver SBRT is not widely discussed in publications. Further, the impact of calculation grid size on dose calculation accuracy is vital in the SBRT of HCC, where thin CT slice thickness (1.25 mm) is used and high dose fall-off to normal liver while achieving adequate dose coverage to the target volume is expected. Furthermore, the use of high-definition multi-leaf collimators (HD-MLC) and flattening filter-free (FFF) beams have been increase the level of concern regarding the dose computation accuracy.

In Eclipse TPS (Varian Medical System, CA, USA), the dose calculation is usually performed using an Anisotropic Analytical Algorithm (AAA) with a range of calculation gird sizes from 1 to 5 mm. Further, VMAT optimization algorithm (Photon optimizer) in the TPS has also includes different resolution settings, viz. fine (1.25 mm), normal (2.5 mm) for dose computation during optimization. The impact of these settings is not being widely debated. Thus, this study is focused on determining an appropriate resolution setting for optimization and dose calculation in VMAT based SBRT using FFF beams for HCC.

Materials and Methods

Patient preparation

CT image set of fifteen HCC patients who already received SBRT at our institution were retrospectively selected for this study. The selection criteria include small sized tumors of primary and metastatic liver, and portal vein tumor thrombosis (PVTT). The median age of these patients was 66 years (range 57 – 81). The informed consent has been waived off by the ethics board of the institution considering this as a retrospective study with no human involved. Patients were immobilized in a supine position using a customized vacuum cushion. Their hands were elevated above the head and kept on a wing board. Abdominal and/or thoracic compression were used to control respiratory movements. Triple phase planning CT images were acquired with a 1.25 mm slice thickness. The CT data sets were imported into Eclipse TPS version 18 (Varian Medical Systems, Palo Alto, CA, USA).

Contouring

The gross tumor volume (GTV) was contoured as the contrast enhanced tumor volume on the triple phase CT scan. In addition, positron emission tomography (PET-CT) and magnetic resonance imaging (MRI) scans were used for GTV delineation. The GTV was expanded to 2–3 mm to generate planning target volume (PTV). The PTV was cropped nearer to any organs at risk (OARs). The OARs were delineated, including normal liver (whole liver minus PTV), stomach, spleen, duodenum, bowel bag, ribs, spinal cord, skin (a 5 mm inner wall from the body surface), and normal tissue (NT), defined as the entire body volume minus PTV. The delineation of PTV and OARs was executed by an experienced radiation oncologist.

Treatment Planning

The SBRT plans were created in the Eclipse TPS using 6X-FFF and 10X-FFF MV photon beams of Truebeam STx linear accelerator (Varian Medical System, CA, USA) furnished with a HD-MLC. The PTV was prescribed by a hypofractionated dose of 50 Gy (10 Gy per fraction) in 5 fractions. For all planning, a single isocenter was placed longitudinally at the center of PTV and medially towards the center of the body as illustrated in Figure 1. The VMAT plans utilized two coplanar partial arcs as displayed in Figure 1. Arc1 rotated clockwise from 181° to 40° with 20° collimator angle and arc2 rotated counter-clockwise from 40° to 181° with 350° collimator angle.

The VMAT optimizations were performed using photon optimizer (PO) algorithm with 1.25 and 2.5 mm resolution settings. The optimization dose constraints were almost similar for all plans. The volume dose was computed for both optimization resolution settings using AAA with 1.25 and 2.5 mm dose grid matrix. All individual plans were normalized in such a way that 95% of PTV should receive 100% prescribed dose. Totally 4 plans were created for each energy with the combination of optimization (O) and calculation (C) resolutions viz. O1.25-C1.25, O1.25-C2.5, O2.5-C1.25, O2.5-C2.5. The optimization and calculation times were noted for comparison among all plans. To avoid inter planner variability, all plans were performed by an experienced medical physicist.

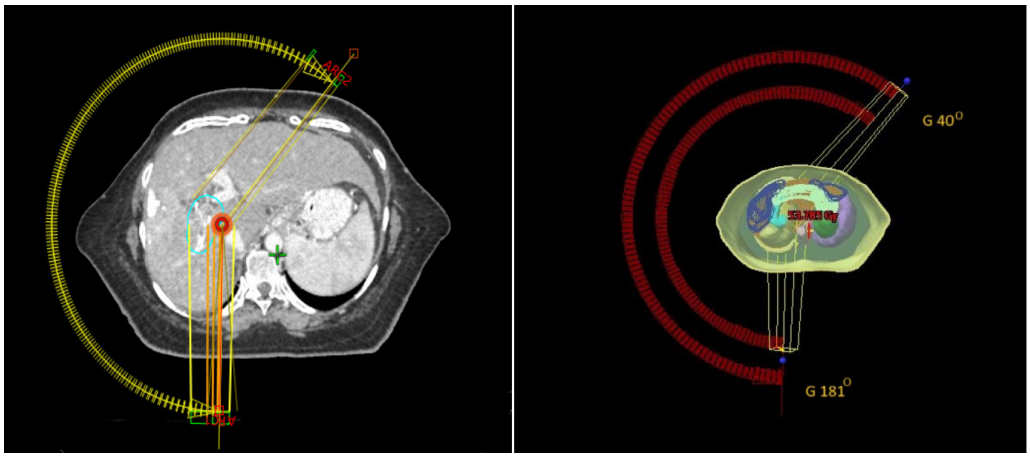

Figure 1. Location of Isocenter and Arc Field Arrangement

Phantom study for delivery efficiency

To estimate the dose variation in the irradiated volume with variable combinations of optimization and calculation grid sizes, a PTV was delineated in an OCTAVIUS-1500 phantom inserted with a 2D-array (PTW-Freiburg, Germany). The CT images of OCTAVIOUS-1500 phantom had been acquired with a 1.25 mm slice thickness. Similar to the patient study, 4 plans were created for each energy with the combination of optimization (O) and calculation (C) resolutions viz. O1.25-C1.25, O1.25-C2.5, O2.5-C1.25, O2.5-C2.5. The plans were delivered to the OCTAVIOUS-1500 phantom with 2D-array setup and the calculated central axis doses were compared with the measured doses. Further, Gamma agreement index (GAI) analysis was performed with 2% dose difference and 1 mm distance to agreement criteria and a tolerance level of 90% [15].

Plan evaluation

The PTV and OARs dosimetric evaluation of these SBRT plans had been made using dose-volume histogram (DVH) analysis. For the PTV quality comparison, dosimetric indices like coverage index (COI), conformity index (CI), uniformity index (UI), gradient index (GI), and gradient measure (GM) were calculated as stated below. The COI was defined as:

$$\mathrm{COI} = \frac{D_P}{D_{98\%}},$$

where D_p is the prescription dose and $D_{98\%}$ is the dose received by 98% of the PTV. The CI was calculated as:

$$\mathrm{CI} = \frac{V_{PTV}}{V_{PTVref}} \times \frac{V_{ref}}{V_{PTVref}},$$

where V_{PTV} is the volume of PTV, V_{PTVref} is the reference isodose (98%) volume within the PTV, and V_{ref} is the volume of reference isodose (98%). The UI was calculated as:

$$\mathrm{UI} = \frac{D_{2\%}}{D_{98\%}},$$

where $D_{2\%}$, $D_{98\%}$ are the doses received by 2%, 98% of the PTV respectively. The GI was defined as:

$$\mathrm{GI} = \frac{V_{50\%}}{V_{PTV}},$$

where $V_{50\%}$ is 50% isodose volume and V_{PTV} is the volume of PTV. Further, the GM is defined as the difference between the equivalent sphere radius of the 100% and 50% isodoses.

The ideal value for COI, CI, UI, GI, and GM is 1 and, a plan with a value closer to 1 indicates a superior plan. The tolerance dose for all OARs was listed in Table 1 for comparison [16]. In addition, total monitor units (MU) and beam-on time (BOT) were noted to assess the delivery efficiency. Further, the phantom study measurement results were compared with TPS calculated doses and GAI analysis results were compared among all generated plans.

A simple plan quality scoring method by Balaji et al. was utilized to calculate an overall score that incorporates all dosimetric parameters evaluated [17]. The overall score was calculated as:

$$\text{Overall Score} = \frac{\sum_{i=1}^{n} \left(\frac{A_i}{D_i}\right)}{n}$$

where A_i is an achieved value of the i^{th} dosimetric index of a particular plan and D_i is the desired value i^{th} dosimetric index and n is a number of dosimetric indices assessed. In contrast, the formula uses D_i / A_i for dosimetric parameters (volume of normal liver that receives less than 21.5 Gy and GAI), where a higher value is better. For all the dosimetric indices, their average of achieved values from all plans were taken as the desired values. A plan that shows the lowest overall score is titled a superior plan.

Statistical analysis

The dosimetric results of all plans were analyzed using the non-parametric Kruskal-Wallis test used for non-normally distributed data from three or more independent groups' comparison. The statistical test was two-tailed, with a threshold for statistical significance of $p < 0.05$.

Results

The mean ± standard deviation (SD) of volumes of PTV and normal liver were 54.63 ± 36.14, and 1289.94 ± 303.95 cm^3 respectively. The PTV parameter results for all SBRT plans are summarized in Table 2. The 95% and 50% dose distribution comparison among all plans of a sample case were illustrated in Figure 2. The SBRT plans achieved anticipated PTV coverage (COI ≤ 1.02), and there were no statistically significant differences among the plans ($p = 0.4024$). The CI and UI of the PTV has shown statistical significance among all SBRT plans (CI: $p = 0.0021$ and UI: $p < 0.0001$). The GI and GM of the PTV have shown comparable results among all SBRT plans (GI: $p = 0.8380$ and GM: $p = 0.5002$).

Table 3 & 4 summarizes the OARs dosimetric comparison results of all SBRT plans. The OARs dose parameters were showed no statistically significant differences among the SBRT plans ($p > 0.402$) except the maximum dose to skin. The skin maximum doses were significantly less in 10X-FFF plans compared to 6X-FFF plans ($p = 0.0007$).

Table 1. Tolerance Dose Limits for All Organs at Risk

Organs at risk	Dose limits
Bowel Bag	$D_{Max} \leq 35$ Gy
Duodenum	$D_{Max} \leq 35$ Gy
Normal Liver	$RV_{21.5Gy} \geq 700$ cm^3; $D_{Mean} \leq 13$ Gy
NT	$D_{Mean} \leq 2$ Gy
Ribs	$D_{Max} \leq 57$ Gy
Skin	$D_{Max} \leq 38.5$ Gy
Spinal cord	$D_{Max} \leq 28$ Gy
Spleen	$D_{Max} \leq 35$ Gy
Stomach	$D_{Max} \leq 35$ Gy

NT, Normal tissue; Gy, gray; $RV_{21.5Gy}$, The volume of normal liver that receives less than 21.5 Gy dose; D_{Mean}, Mean dose; D_{Max}, Maximum dose

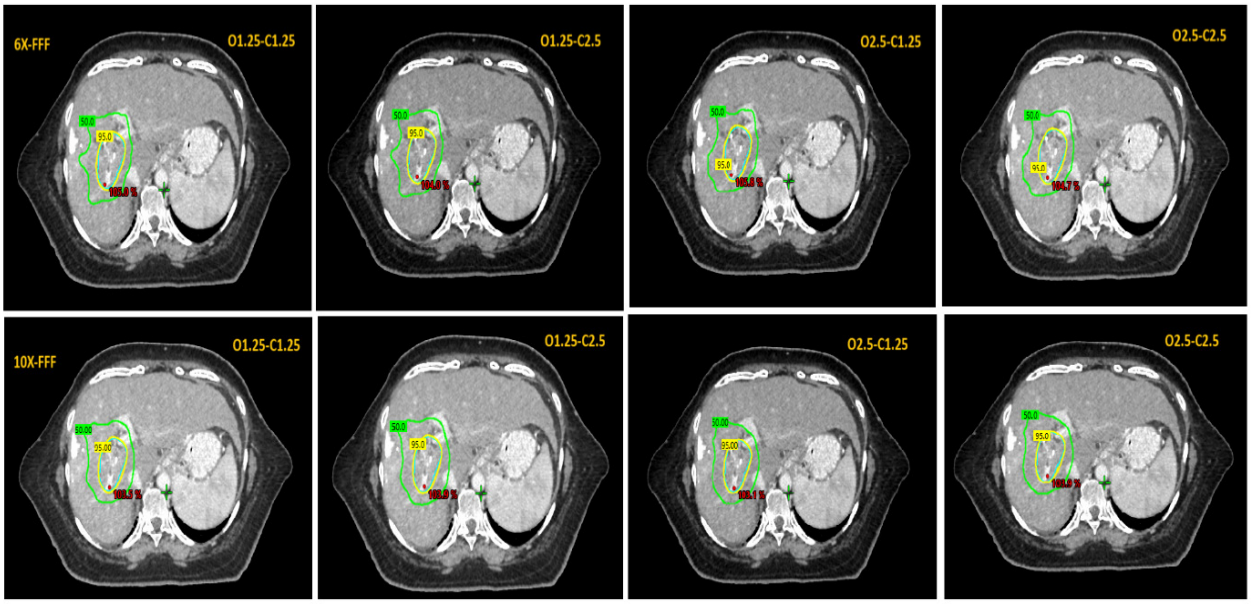

Figure 2. Comparison of Dose Distribution among All Plans

The OCTAVIOUS-1500 phantom study results, MU, BOT, optimization, and calculation times were presented in the Table 5. The MU and BOT were significantly less in the 10X-FFF plans compared to 6X-FFF plans ($p < 0.00001$). The optimization and calculation times were significantly less in 2.5 mm resolution setting compared to 1.25 mm ($p < 0.00001$). The O1.25-C1.25 plan provided better point dose result among 6X-FFF plans, while the O2.5-C2.5 plan provided better point dose result among 10X-FFF plans. Further, the O2.5-C2.5 plan provided better GAI result among 6X-FFF plans as well as10X-FFF plans.

The integrated plan quality scores that incorporated all dosimetric parameters of PTV and OARs and excluded the optimization and calculation times were 1.042, 1.026, 1.001, and 1.001 for O1.25-C1.25, O1.25-C2.5, O2.5-C1.25, and O2.5-C2.5 6X-FFF plans respectively. Similarly, the integrated plan quality scores were 0.997, 0.933, 1.059, and 0.988 for O1.25-C1.25, O1.25-C2.5, O2.5-C1.25, and O2.5-C2.5 10X-FFF plans respectively. The integrated score revealed that the O1.25-C1.25 10X-FFF plan provided better results for OARs compared to other plans. Nevertheless, the O2.5-C2.5 10X-FFF plan provided better results if the integrated score calculation includes the optimization and calculation times. This is due to significant reduction in the optimization and calculation times in this plan.

Discussion

Achieving an accurate volume dose computation for liver SBRT is crucial due to the involvement of various facts like irradiation of small field, thin slice CT image, HD-MLC leaf width, hypofractionated dose,

Table 2. Dosimetric Parameters Results for Planning Target Volume

Parameter	COI	CI	UI	GI	GM (cm)
6X-FFF					
O1.25-C1.25	1.012 ± 0.005	1.210 ± 0.070	1.064 ± 0.010	3.694 ± 0.465	1.405 ± 0.351
O1.25-C2.5	1.011 ± 0.003	1.148 ± 0.031	1.053 ± 0.013	3.710 ± 0.393	1.355 ± 0.278
O2.5-C1.25	1.012 ± 0.006	1.208 ± 0.083	1.062 ± 0.010	3.708 ± 0.427	1.411 ± 0.348
O2.5-C2.5	1.011 ± 0.004	1.150 ± 0.032	1.053 ± 0.012	3.739 ± 0.410	1.371 ± 0.288
p1 value	0.3541	0.0012#	0.0010#	0.9370	0.9141
10X-FFF					
O1.25-C1.25	1.010 ± 0.003	1.164 ± 0.044	1.046 ± 0.013	3.622 ± 0.478	1.335 ± 0.236
O1.25-C2.5	1.010 ± 0.004	1.146 ± 0.026	1.052 ± 0.014	3.707 ± 0.479	1.265 ± 0.227
O2.5-C1.25	1.010 ± 0.003	1.167 ± 0.037	1.046 ± 0.013	3.643 ± 0.465	1.388 ± 0.259
O2.5-C2.5	1.010 ± 0.004	1.150 ± 0.030	1.051 ± 0.014	3.726 ± 0.472	1.276 ± 0.237
p2 value	0.5112	0.5011	0.2957	0.6622	0.3688
pA value*	0.4024	0.0021#	< 0.0001#	0.8380	0.5002

COI, Coverage index; CI, Conformity index; UI, Uniformity index; GI, Gradient index; GM, Gradient measure; p1, p value for 6X-FFF plans; p2, p value for 10X-FFF plans; pA, p value for all plans; *, Kruskal-Wallis test; #, Statistically significant result

Table 3. Comparison Results of Organs at Risk Dosimetric Parameters

Parameter	Bowel bag D_{Max} (Gy)	Duodenum D_{Max} (Gy)	Normal liver $RV_{21.5Gy}$ (cm^3)	Normal liver D_{Mean} (Gy)	NT D_{Mean} (Gy)
6X-FFF					
O1.25-C1.25	6.72 ± 6.74	4.66 ± 10.76	1101.33 ± 231.27	8.22 ± 2.51	1.40 ± 0.67
O1.25-C2.5	6.68 ± 6.70	4.70 ± 10.78	1100.22 ± 231.98	8.28 ± 2.55	1.41 ± 0.68
O2.5-C1.25	6.20 ± 6.06	4.70 ± 11.09	1097.69 ± 230.23	8.20 ± 2.38	1.39 ± 0.66
O2.5-C2.5	6.22 ± 6.07	4.72 ± 11.01	1096.11 ± 231.88	8.33 ± 2.53	1.42 ± 0.68
p1 value	0.9982	0.9826	0.9799	0.9231	0.9761
10X-FFF					
O1.25-C1.25	6.14 ± 5.78	4.55 ± 11.14	1103.60 ± 230.86	8.07 ± 2.49	1.35 ± 0.66
O1.25-C2.5	6.09 ± 5.87	4.63 ± 11.23	1099.78 ± 231.97	8.21 ± 2.54	1.37 ± 0.68
O2.5-C1.25	6.45 ± 6.44	4.61 ± 11.24	1104.03 ± 230.93	8.11 ± 2.49	1.35 ± 0.66
O2.5-C2.5	6.48 ± 6.41	4.68 ± 11.27	1100.42 ± 231.90	8.24 ± 2.53	1.38 ± 0.67
p2 value	0.9998	0.9792	0.9591	0.9566	0.9501
pA value*	1.0000	0.9931	0.9996	0.9908	0.9957

NT, Normal tissue; Gy, gray; D_{Mean}, Mean dose; D_{Max}, Maximum dose; $RV_{21.5Gy}$, The volume of normal liver that receives less than 21.5 Gy dose; p1, p value for 6X-FFF plans; p2, p value for 10X-FFF plans; pA, p value for all plans; *, Kruskal-Wallis test

and the involvement of FFF photon beams. Published studies have shown that the dose calculation accuracy is influenced by calculation grid size. The goal of this dosimetric comparison study is to establish an appropriate resolution setting for optimization and dose calculation for liver SBRT.

Advanced TPS is warranted to get accurate dose calculation for liver SBRT where various influencing factors are involved. Prior to this study we calculated open field dose to check the impact of calculation grid size of AAA in the Eclipse TPS. Both 6X-FFF and 10X-FFF beams were calculated with 1.25 mm and 2.5 mm calculation grid sizes for a dose of 5 Gy deliverable using 5 cm open field and 10 cm depth in the OCTAVIUS-1500 phantom. Between the two resolutions a difference of 1 MU was found to deliver an open field dose of 5 Gy.

Clinically, the impact of dose calculation resolutions on the calculated doses was more pronounced in maximum dose to the OARs those are proximity to the PTV. Published studies have recommended diverse calculation grid sizes. For instance, Park et al. evaluated VMAT plans with different calculation grid sizes ranging from 1 to 5 mm for brain, orbit, and head & neck patients [13]. They recommended a calculation grid size of 2 mm to protect eye lenses and optic pathways using AAA in Eclipse TPS. In a small fields study, Ong et al. suggested 1 mm calculation grid size of AAA for VMAT plans [9]. Snyder Karen et al. dosimetrically compared 1 mm, 1.5 mm, and 2.5 mm resolutions of AAA for spine SBRT using VMAT technique [12]. They concluded that the use of a 1.5 mm calculation grid size balances accurate spinal cord dose and PTV coverage. In a lung SBRT study, Park et al. compared AAA calculation grid sizes of 2 mm, 3 mm, and 4 mm using dynamic conformal arc therapy (DCAT).

Table 4. Comparison Results of Organs at Risk Dosimetric Parameters

Parameter	Ribs D_{Max} (Gy)	Skin D_{Max} (Gy)	Spinal cord D_{Max} (Gy)	Spleen D_{Max} (Gy)	Stomach D_{Max} (Gy)	Overall Score
6X-FFF						
O1.25-C1.25	27.90 ± 10.03	18.44 ± 4.76	6.89 ± 2.47	5.21 ± 1.51	11.85 ± 9.53	1.049
O1.25-C2.5	27.74 ± 10.16	18.18 ± 4.71	6.83 ± 2.43	5.20 ± 1.49	11.84 ± 9.70	1.000
O2.5-C1.25	28.15 ± 10.12	18.80 ± 4.47	6.72 ± 2.46	5.51 ± 1.68	12.00 ± 9.37	1.041
O2.5-C2.5	28.02 ± 10.37	18.63 ± 4.59	6.62 ± 2.40	5.43 ± 1.62	11.93 ± 9.49	0.978
p1 value	0.9821	0.9709	0.9599	0.9481	0.9970	
10X-FFF						
O1.25-C1.25	27.42 ± 10.69	13.93 ± 3.53	7.24 ± 2.27	5.74 ± 1.24	11.94 ± 9.48	1.059
O1.25-C2.5	27.61 ± 10.93	13.84 ± 3.50	7.28 ± 2.30	5.79 ± 1.26	12.00 ± 9.72	0.988
O2.5-C1.25	27.57 ± 10.76	14.26 ± 3.73	7.27 ± 2.32	5.93 ± 1.34	11.72 ± 8.92	0.997
O2.5-C2.5	27.63 ± 10.92	14.24 ± 3.76	7.31 ± 2.36	5.96 ± 1.35	11.81 ± 9.12	0.933
p2 value	0.9997	0.9549	0.9983	0.9523	0.9999	
pA value*	0.9993	0.0007#	0.9159	0.7974	1.0000	

Gy, gray; D_{Max}, Maximum dose; p1, p value for 6X-FFF plans; p2, p value for 10X-FFF plans; pA, p value for all plans; *, Kruskal-Wallis test; #, Statistically significant result

Table 5. Comparison Results of Phantom Study for Delivery Efficiency

Parameter	Optimization time (min)	Calculation time (min)	MU	BOT (min)	Point dose difference (%)	GAI (%)
6X-FFF						
O1.25-C1.25	46.44 ± 11.70	6.21 ± 0.97	2523.5 ± 246.5	2.07 ± 0.19	-0.71	93.9
O1.25-C2.5	46.44 ± 11.70	2.06 ± 0.35	2540.8 ± 243.0	2.08 ± 0.19	-0.81	95.5
O2.5-C1.25	17.07 ± 3.75	6.21 ± 1.16	2606.1 ± 161.5	2.11 ± 0.13	-1.41	93.9
O2.5-C2.5	17.07 ± 3.75	2.05 ± 0.39	2568.7 ± 168.5	2.09 ± 0.14	-1.25	96.1
p1 value	< 0.0001#	< 0.0001#	0.4187	0.4187	NA	NA
10X-FFF						
O1.25-C1.25	46.74 ± 11.46	6.07 ± 0.83	2319.2 ± 164.8	1.79 ± 0.00	-1.62	94.8
O1.25-C2.5	46.74 ± 11.46	2.04 ± 0.29	2359.2 ± 165.8	1.79 ± 0.00	-1.09	95.9
O2.5-C1.25	15.90 ± 3.43	6.04 ± 0.69	2266.3 ± 198.5	1.79 ± 0.00	-1.19	96.1
O2.5-C2.5	15.90 ± 3.43	1.99 ± 0.37	2303.9 ± 199.8	1.79 ± 0.00	-0.83	96.8
p2 value	< 0.0001#	< 0.0001#	0.3612	1.0000	NA	NA
pA value*	< 0.0001#	< 0.0001#	< 0.0001#	< 0.0001#	NA	NA

MU, Monitor unit; BOT, Beam-on time; GAI, Gamma agreement index; p1, p value for 6X-FFF plans; p2, p value for 10X-FFF plans; pA, p value for all plans; *, Kruskal-Wallis test; #, Statistically significant result; NA, Not applicable

They concluded that the 3 mm grid size is found to be appropriate for predicting patient dose distributions while reducing the computation time [11].

The present study showed that the 10X-FFF beams provided better results compared to 6X-FFF. This is due to the significant reduction in the skin maximum dose, MU, and BOT. The dosimetric differences, while statistically significant in some cases, are often numerically small and do not show any clinical significance. In this study, the CI values among 6X-FFF plans showed statistically significant results even with the absolute differences of ~0.06. This shows the gap between the statistical results and their practical impact on patient care. With respect to resolution, the integrated scoring method revealed that the 1.25 mm optimization and 1.25 mm calculation grid sized plan achieved better results for OARs, while 1.25 mm optimization and 2.5 mm calculation grid sized plan attained improved outcomes for PTV dosimetric indices among 10X-FFF plans. The MU was lesser in 2.5 mm optimization and 1.25 mm calculation grid sized 10X-FFF plan. Further, it is obvious that the optimization and calculation times were significantly less with 2.5 mm resolution plans.

The OCTAVIUS-1500 phantom study revealed that the delivery accuracy was better in 2.5 mm optimization and 2.5 mm calculation grid size plan. This showed that the 2.5 mm plan utilized a less modulation complexity that delivered a smooth and accurate plan. Nevertheless, all the plans compared in this study provided acceptable delivery accuracy with an absolute dose difference of less than 2% and GAI of greater than 90%.

The exclusion of the impact of calculation grid size in non-coplanar arcs of VMAT was the limitation of this study. Therefore, further investigation is required, which includes the influence of optimization and calculation resolutions with non-coplanar arcs.

In conclusion, though the Eclipse TPS shows the standard resolution setting of 1.25 mm for SBRT, the appropriate resolution setting can be efficiently determined based on the balance between the achieved dose to OARs those are proximity to the PTV and the time consumption for both optimization and dose calculation. Under these circumstances, one can consider 1.25 mm resolution for both optimization and calculation if the critical organs are in priority otherwise 2.5 mm resolution setting will be the optimal choice for liver SBRT using the 10X-FFF photon beam. Since the 10X-FFF beam demonstrated superior efficiency and lower skin dose, the resolution recommendations are primarily made for this energy, which is the preferred choice for liver SBRT based on this study's results.

Author Contribution Statement

M.T. developed performed the treatment plans, analyzed the data and wrote the manuscript. D.K. contributed to the manuscript and supervised the project. K.B and M.R discussed the results and contributed to the manuscript.

Acknowledgements

Ethical Approval

Institutional ethics board has approved this study. This article does not contain any studies with human participants performed by any of the authors.

The informed consent has been waived off by the ethics board of the institute considering this as a retrospective study with no human involved.

Availability of data

The data are available from the corresponding author upon reasonable request.

Conflict of interest

All authors contributed to this study declare that they

have no conflict of interest with respect to the manuscript.

References

1. Bray F, Laversanne M, Sung H, Ferlay J, Siegel RL, Soerjomataram I, et al. Global cancer statistics 2022: Globocan estimates of incidence and mortality worldwide for 36 cancers in 185 countries. CA Cancer J Clin. 2024;74(3):229-63. https://doi.org/10.3322/caac.21834.
2. Høyer M, Swaminath A, Bydder S, Lock M, Méndez Romero A, Kavanagh B, et al. Radiotherapy for liver metastases: A review of evidence. Int J Radiat Oncol Biol Phys. 2012;82(3):1047-57. https://doi.org/10.1016/j.ijrobp.2011.07.020.
3. Doi H, Beppu N, Kitajima K, Kuribayashi K. Stereotactic body radiation therapy for liver tumors: Current status and perspectives. Anticancer Res. 2018;38(2):591-9. https://doi.org/10.21873/anticanres.12263.
4. Huertas A, Baumann AS, Saunier-Kubs F, Salleron J, Oldrini G, Croisé-Laurent V, et al. Stereotactic body radiation therapy as an ablative treatment for inoperable hepatocellular carcinoma. Radiother Oncol. 2015;115(2):211-6. https://doi.org/10.1016/j.radonc.2015.04.006.
5. Jang WI, Bae SH, Kim MS, Han CJ, Park SC, Kim SB, et al. A phase 2 multicenter study of stereotactic body radiotherapy for hepatocellular carcinoma: Safety and efficacy. Cancer. 2020;126(2):363-72. https://doi.org/10.1002/cncr.32502.
6. Mahadevan A, Blanck O, Lanciano R, Peddada A, Sundararaman S, D'Ambrosio D, et al. Stereotactic body radiotherapy (sbrt) for liver metastasis - clinical outcomes from the international multi-institutional rssearch® patient registry. Radiat Oncol. 2018;13(1):26. https://doi.org/10.1186/s13014-018-0969-2.
7. Scorsetti M, Comito T, Clerici E, Franzese C, Tozzi A, Iftode C, et al. Phase ii trial on sbrt for unresectable liver metastases: Long-term outcome and prognostic factors of survival after 5 years of follow-up. Radiat Oncol. 2018;13(1):234. https://doi.org/10.1186/s13014-018-1185-9.
8. Sapkaroski D, Osborne C, Knight KA. A review of stereotactic body radiotherapy - is volumetric modulated arc therapy the answer? J Med Radiat Sci. 2015;62(2):142-51. https://doi.org/10.1002/jmrs.108.
9. Ong CL, Cuijpers JP, Senan S, Slotman BJ, Verbakel WF. Impact of the calculation resolution of aaa for small fields and rapidarc treatment plans. Med Phys. 2011;38(8):4471-9. https://doi.org/10.1118/1.3605468.
10. Huang B, Wu L, Lin P, Chen C. Dose calculation of acuros xb and anisotropic analytical algorithm in lung stereotactic body radiotherapy treatment with flattening filter free beams and the potential role of calculation grid size. Radiat Oncol. 2015;10:53. https://doi.org/10.1186/s13014-015-0357-0.
11. Park JY, Kim S, Park HJ, Lee JW, Kim YS, Suh TS. Optimal set of grid size and angular increment for practical dose calculation using the dynamic conformal arc technique: A systematic evaluation of the dosimetric effects in lung stereotactic body radiation therapy. Radiat Oncol. 2014;9:5. https://doi.org/10.1186/1748-717x-9-5.
12. Snyder Karen C, Liu M, Zhao B, Huang Y, Ning W, Chetty IJ, et al. Investigating the dosimetric effects of grid size on dose calculation accuracy using volumetric modulated arc therapy in spine stereotactic radiosurgery. J Radiosurg SBRT. 2017;4(4):303-13.
13. Park JM, Park SY, Kim JI, Carlson J, Kim JH. The influence of the dose calculation resolution of vmat plans on the calculated dose for eye lens and optic pathway. Australas Phys Eng Sci Med. 2017;40(1):209-17. https://doi.org/10.1007/s13246-016-0517-z.
14. Chung H, Jin H, Palta J, Suh TS, Kim S. Dose variations with varying calculation grid size in head and neck imrt. Phys Med Biol. 2006;51(19):4841-56. https://doi.org/10.1088/0031-9155/51/19/008.
15. Kim JI, Chun M, Wu HG, Chie EK, Kim HJ, Kim JH, et al. Gamma analysis with a gamma criterion of 2%/1 mm for stereotactic ablative radiotherapy delivered with volumetric modulated arc therapy technique: A single institution experience. Oncotarget. 2017;8(44):76076-84. https://doi.org/10.18632/oncotarget.18530.
16. Timmerman R. A story of hypofractionation and the table on the wall. Int J Radiat Oncol Biol Phys. 2022;112(1):4-21. https://doi.org/10.1016/j.ijrobp.2021.09.027.
17. Balaji K, Ramasubramanian V. Integrated scoring approach to assess radiotherapy plan quality for breast cancer treatment. Rep Pract Oncol Radiother. 2022;27(4):707-16. https://doi.org/10.5603/RPOR.a2022.0083.